Article

Growth and Structure of Rare-Earth Molybdate Crystals Na$_{0.65}$La$_{4.35}$Mo$_3$O$_{15.81\pm\delta}$F$_{0.07\pm\varepsilon}$

Nataliya E. Novikova [1],*, Ekaterina I. Orlova [1,2,*], Alexander M. Antipin [1], Timofei A. Sorokin [1], Vladimir B. Kvartalov [1], Elena P. Kharitonova [1,2], Nataliya I. Sorokina [1], Olga A. Alekseeva [1] and Valentina I. Voronkova [2]

[1] Shubnikov Institute of Crystallography, Federal Scientific Research Centre "Crystallography and Photonics" of Russian Academy of Sciences, Leninskiy Prospekt 59, 119333 Moscow, Russia; antipin@physics.msu.ru (A.M.A.); tim29@inbox.ru (T.A.S.); kvartalov@gmail.com (V.B.K.); harit@polly.phys.msu.ru (E.P.K.); nsor@ns.crys.ras.ru (N.I.S.); olalex@crys.ras.ru (O.A.A.)
[2] Faculty of Physics, Lomonosov Moscow State University, GSP-1, Leninskiye Gory, 119991 Moscow, Russia; voronk@polly.phys.msu.ru
*   Correspondence: nata110565@mail.ru (N.E.N.); agapova@polly.phys.msu.ru (E.I.O.); Tel.: +7-499-135-31-10 (N.E.N.); +7-495-939-28-83 (E.I.O.)

Abstract: Rare-earth sodium- and fluorine-substituted molybdates with the Na$_{0.65}$La$_{4.35}$Mo$_3$O$_{15.81\pm\delta}$F$_{0.07\pm\varepsilon}$ composition were synthesized for the first time as single crystals. An accurate X-ray diffraction analysis of three samples at room temperature showed that the obtained crystals are isostructural to undoped cubic compounds of the Ln_5Mo$_3$O$_{16+\delta}$ family (space group $Pn\bar{3}n$). Sodium cations partially occupy one of the two lanthanum positions and center the more distorted LaO$_8$ polyhedra, while fluorine anions occupy over-stoichiometric oxygen positions in the vast interstices (cavities) of the structure. The partial substitution of fluorine atoms for oxygen ones affects the transport characteristics of compounds by activating the oxygen atoms in the anionic subsystem due to the effect of supplementary electrostatic repulsion between anions of different types.

Keywords: rare-earth molybdates; crystal growth; crystal structure; fluorine-containing molybdates; oxyfluorides; Nd$_5$Mo$_3$O$_{16}$; NaLa$_4$Mo$_3$O$_{15}$F

1. Introduction

The class of rare-earth cubic molybdates Ln_5Mo$_3$O$_{16+\delta}$ (Ln = La–Gd) [1] is of interest due to the high mixed oxygen ion and electronic conductivity of these crystals, which reaches 10^{-2} S cm^{-1} at 700 °C [2,3]. Such materials can be used in electrochemical instruments, for example, as anodes in solid oxide fuel cells [4–6].

The group of compounds Ln_5Mo$_3$O$_{16}$, where Ln = La, Pr, Nd, Sm, isomorphic to the fluorite-like compound CdTm$_4$Mo$_3$O$_{16}$ [7,8], was first described by Hubert et al. [1]. It has been noted that the Ln_5Mo$_3$O$_{16}$ phases obtained under reducing conditions can be heated in air without changing the structure, although the oxygen content changes; therefore, the composition of the phases can be expressed as Ln_5Mo$_3$O$_{16+\delta}$, where δ = 0–0.5 [1,2].

The structure of the family of compounds Ln_5Mo$_3$O$_{16+\delta}$ was first solved in [1] and later refined in a number of works [9,10]. According to [1], in the structure of Nd$_5$Mo$_3$O$_{16}$ (space group $Pn\bar{3}n$), there are five independent crystallographic atomic positions: Nd1, Nd2, Mo, O1, and O2 atoms, with the positions of oxygen atoms O1 and O2 being completely occupied. The Mo atom is coordinated by four O2 atoms. The preferred tetrahedral coordination of molybdenum atoms is realized (Figure 1a). The MoO$_4$ tetrahedra in the structure have neither common vertices nor common faces; their vertices connect the polyhedra of rare-earth cations into a framework (Figure 1b). The Nd1 atom is surrounded by four O1 and four O2 atoms, and the Nd2 atom is coordinated by two O1 and six O2 atoms; the Nd1O$_8$ and Nd2O$_8$ polyhedra are distorted cubes. The anion lattice is deformed;

this is necessary to ensure the coordination, which is characteristic of rare-earth elements (CN = 8) and molybdenum (CN = 4) (CN is the coordination number) under the "fluorite" law of their arrangement in the crystal structures of binary oxide phases [9]. Due to this configuration of cations and deformation of the lattice of oxygen atoms, vast cavities (interstices) are formed in the structure. It was noted in [9] that since there are no oxygen vacancies in the structure of the reduced $Ln_5Mo_3O_{16}$ compound, over-stoichiometric oxygen atoms in a $Ln_5Mo_3O_{16+\delta}$ sample annealed in air can be located in these interstices.
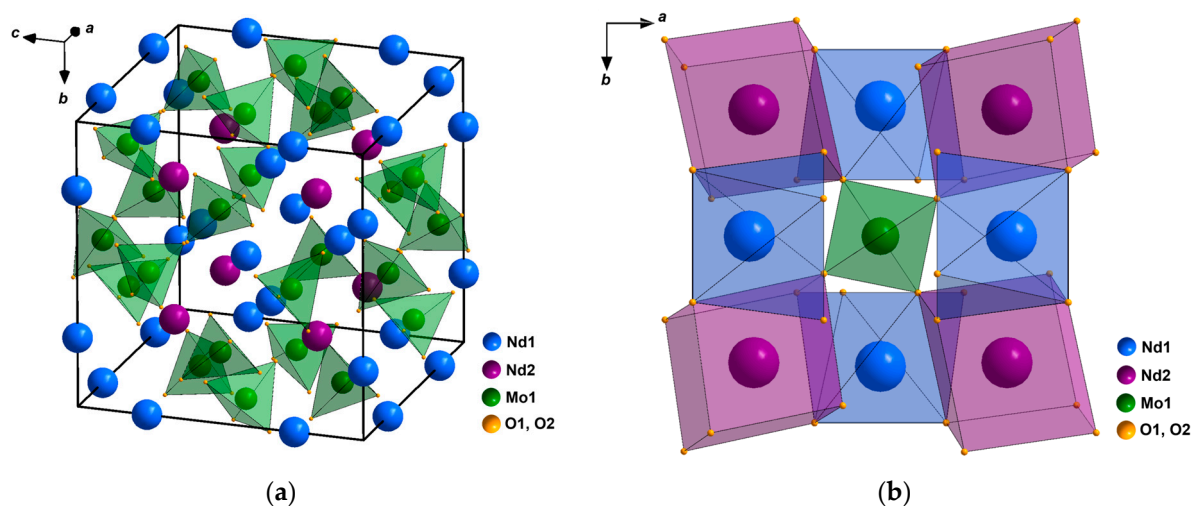

(a)   (b)

Figure 1. Structure of a $Nd_5Mo_3O_{16}$ single crystal: (**a**) Unit cell; (**b**) Framework fragment in which each molybdenum tetrahedron links eight distorted neodymium cubes.

The family of $Ln_5Mo_3O_{16+\delta}$ compounds can be extended by heterovalent doping, as shown in [11–14]. Anion doping is of particular interest; it allows one to change the structure of materials and transport characteristics.

The effect of partial fluorine substitution for oxygen on the conductivity of complex oxides has been extensively studied previously for compounds of various structural types, including brownmillerite [15,16], perovskite [17,18], and potassium titanyl phosphate [19]. In particular, the introduction of a small amount of fluorine into compounds based on brownmillerite $Ba_2In_2O_5$ [15] led to an increase in oxygen ion conductivity due to the effects of electrostatic repulsion of oxygen and fluorine ions in the anionic lattice. In addition, it was found in [15,17,18] that the proton component of conductivity was present in fluorine-substituted phases with perovskite and brownmillerite structures at temperatures below 700 °C in a humid atmosphere. It was noted in [20] that in the $SrFeO_{3-\delta}$ compound, the partial replacement of oxygen by halogens (fluorine or chlorine) led to a significant increase in oxygen conductivity in the high-temperature phase and increased the stability of ferrite under reducing conditions. In general, these data indicate that the partial fluorine substitution for oxygen can significantly affect the conductivity and stability of complex oxides.

The fluorite-like structure of compounds of the $Ln_5Mo_3O_{16+\delta}$ type is resistant to combined cationic and anionic doping. In a series of works [21,22], ceramics of the composition $MeLn_4Mo_3O_{15}F$ (Me = Li, Na; Ln = La, Pr, Nd, Sm), isostructural to the $Ln_5Mo_3O_{16+\delta}$ phases, were successfully synthesized. It was shown that the fluorination of these materials led to a reversible phase transition, in which the anionic conductivity of the phases sharply increased. In addition to increasing conductivity, combined doping provides another advantage. It stabilizes the molybdate structure. It should be noted that it is impossible to obtain a $La_5Mo_3O_{16}$ compound in air, only under reducing conditions, for example, in evacuated ampoules. This was established by Tsai et al. [2] and also additionally confirmed in our experiments. It is very important to obtain stable compounds with high conductivity in order to further use them in electrochemical devices.

To explain the changes in the physical properties during the fluorination of compounds of the $Ln_5Mo_3O_{16+\delta}$ type, it is necessary to precisely describe their crystal structure. In [23], phases of the nominal composition $LiLa_4Mo_3O_{15}F$ were synthesized for the first time as single crystals, and an accurate X-ray diffraction analysis was carried out at 20 and $-183\,°C$. It was proved that fluorine atoms substituted for over-stoichiometric oxygen atoms in the vast cavities of the framework, affecting the interstitial conductivity of the studied $LiLa_4Mo_3O_{15}F$ phases. It is of interest to continue a series of studies of the crystal structure of rare-earth molybdates containing fluorine. In this work, for the first time, a compound of the nominal composition $NaLa_4Mo_3O_{15}F$ of the $Ln_5Mo_3O_{16+\delta}$ family was synthesized in a single-crystal phase. An accurate X-ray diffraction study of its atomic structure was performed.

2. Materials and Methods

Polycrystalline samples of the nominal composition $NaLa_4Mo_3O_{15}F$ were synthesized by solid-state reactions in air using a stoichiometric mixture of the reagents NaF, La_2O_3, and MoO_3 (99.9%). Before weighing, lanthanum oxide was annealed at $1000\,°C$ for 24 h, and sodium fluoride was annealed at $400\,°C$ for 6 h in order to remove water and carbon dioxide. The two-stage firing of pressed samples was performed at 600 and $700\,°C$ for 12 h.

To grow single crystals of $Na_xLa_{5-x}Mo_3O_{16.5-y}F_y$, the flux method of crystallization was applied. The low melting temperature of the solvent is a necessary condition for the growth of fluorine-containing compounds of the $Ln_5Mo_3O_{16+\delta}$ family since according to [21], at temperatures above 700–800 °C, fluorine sublimation from $NaLa_4Mo_3O_{15}F$ samples takes place. The fusible solvent was chosen in the binary system 80 mol% Na_2MoO_4–20 mol% NaF. To obtain the Na_2MoO_4 compound and maintain the indicated proportion, a mixture of the reagents Na_2CO_3 (80 mol%) and MoO_3 (80 mol%) was used. Thus, a mixture of the reagents Na_2CO_3 (80 mol%), MoO_3 (80 mol%), and NaF (20 mol%) was used as a fusible solvent.

The prior prepared polycrystalline samples of $NaLa_4Mo_3O_{15}F$ weighed approximately 4 g and were placed on the bottom of a 25 mL platinum crucible. The crucible with ceramics was filled with 40 g of a solvent mixture and heated to $720\,°C$ in an oven. When this temperature was reached, the solvent mixture melted and became transparent. As a result, the polycrystalline samples of $NaLa_4Mo_3O_{15}F$ were partially dissolved in the mixture, and the ceramics remaining at the bottom of the platinum crucible served as a seed for the subsequent growth of single crystals. An increase in the melt temperature led to the appearance of numerous bubbles on the surface of the ceramics, indicating the sublimation of fluorine. The maximum possible temperature of the melt was limited to $720\,°C$ since an increase in the temperature led to the sublimation of fluorine.

After holding the melt at $720\,°C$ for a week, it was gradually cooled down at a rate of $1\,°C\,h^{-1}$ until a temperature of $650\,°C$ was reached, at which time it completely solidified. The crucible was then cooled to room temperature at a rate of $50\,°C\,h^{-1}$. The crystals were effortlessly separated from the solvent by washing them with hot water. The synthesis products are shown in Figure 2a. Dark yellow cubic crystals of 0.1–0.2 mm in size were obtained as the main phase of $Na_xLa_{5-x}Mo_3O_{16.5-y}F_y$ (Figure 2b).
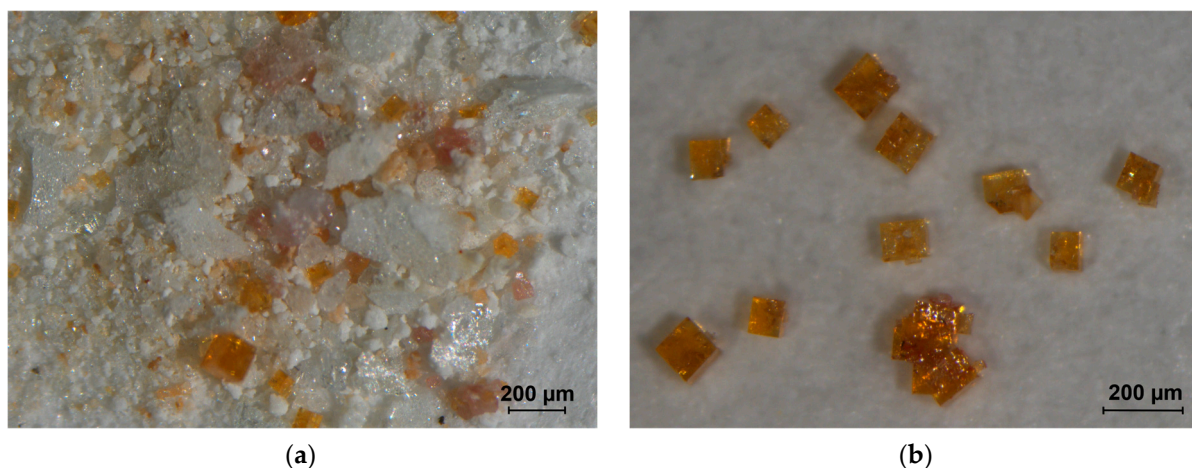
Figure 2. Photograph of $Na_xLa_{5-x}Mo_3O_{16.5-y}F_y$ single crystals illuminated by an LED lamp (5600 K): (**a**) Synthesis products; (**b**) Individual single crystals.

X-ray phase analysis was carried out at room temperature on a Rigaku Miniflex 600 diffractometer (Rigaku Corporation, Tokyo, Japan) (Cu $K\alpha$ radiation, Ni filter). Synthesis products as a mixture of single crystals and polycrystals of various phases served as a sample for the study (Figure 2a). They were ground to a fine-dispersed state in an agate mortar and then placed in a cuvette made of X-ray amorphous quartz. Scanning was performed in the 2θ range 10°–70° in steps of 0.02°. The processing of the diffraction pattern was conducted using the Miniflex Guidance, PDXL-2 (Rigaku Corporation, Tokyo, Japan), Match software package, as well as the ICDD PDF-2 and ICSD/CCDC databases. Quantitative full profile analysis by the Rietveld method was fulfilled using the JANA2006 program [24]. The phase relationships were refined by successively adding refined parameters, starting with the most stable and ending with the correlating ones. At the same time, continuous graphical modeling of the background was carried out until the values of the *R*-factors stabilized.

The concentration of sodium ions was measured by inductively coupled plasma mass spectrometry (ICP-MS method) on an iCapQc mass spectrometer (Thermo Scientific, Bremen, Germany). The single crystals (Figure 2b) selected for the research were decomposed in a mixture of concentrated sulfuric acid (H_2SO_4 98%, EMSURE ISO, Merck, Darmstadt, Germany) (2 mL) and phosphoric acid (H_3PO_4 98%, ACROS, Geel, Belgium) (2 mL) of the appropriate purity in a microwave autoclave at 240 °C for 1.5 h. During sample preparation, a microwave decomposition system CEM Mars 6 and deionized water (residual resistance 18.2 MΩ) were used. Nitric acid of the appropriate purity (HNO_3 65%, EMSURE ISO, Merck, Darmstadt, Germany) was taken for dilution. Calibration was performed using the MS68A multi-element standard set for ICP-MS (68 components). To control the precision of the measurements and the matrix effect, internal standards were used, namely, aliquots of solutions of Sc, In, and Bi cations (2 ppb each).

Three single-crystal samples (Figure 2b) with the best profiles of diffraction peaks and convergence of intensities of symmetrically equivalent reflections were selected for X-ray diffraction experiments. Complete diffraction experiments were carried out at room temperature on an Oxford Diffraction Xcalibur EosS2 diffractometer equipped with a CCD detector. Data reduction was fulfilled using the CrysAlisPro program [25]. The absorption was corrected, allowing for the shapes and sizes of the specimens, with the use of numerical integration in Gaussian [25].

As a result of the search for unit cells of crystals at room temperature, cubic cells were chosen with the parameters $a = 11.2327(1)$ Å for the first sample, $a = 11.2387(1)$ Å for the second sample, and $a = 11.2368(1)$ Å for the third sample.

Obtaining structural data for $Na_xLa_{5-x}Mo_3O_{16.5-y}F_y$ crystals was complicated by the fact that all three samples were intergrowths of single-crystal individuals, the lattices of

which were misoriented relative to each other: they had a common axis and were rotated through a certain angle (Figure 3). The defect structure varied from crystal to crystal. We believe that such defect formation is conditioned by the chosen synthesis method, i.e., using ceramic grains as seed material. It is likely that initially, the growth occurs near the seed, and then with the use of a solvent material, these two stages of growth cause the intergrowth of crystals. In other words, intergrowth is the response of a growing crystal to a change in the crystallization conditions. The compositions of ceramic grains can differ somewhat; therefore, the compositions of grown crystals can also differ slightly, which entails a slight difference in the unit cell parameters observed in experiments. The lattices of individuals in the first and second samples were slightly misoriented (Figure 3a,b). In the case of the first sample, 66.7% of the measured reflections for the first individual and 69.4% for the second individual were indexed, the overlap of the reflections was 47.5%, and in the case of the second sample, 55.1 and 39.7%, respectively, the overlap was 5.7%. In the third sample (Figure 3c), the lattices were rotated by 30° relative to the common axis and were connected by the transformation matrix.

$$\begin{pmatrix} 0.053 & -0.859 & 0.508 \\ -0.025 & -0.510 & -0.859 \\ 0.998 & 0.033 & -0.048 \end{pmatrix}$$

The bases were transformed according to the law:

$$\mathbf{a}_{II} = 0.053\mathbf{a}_I - 0.859\mathbf{b}_I + 0.508\mathbf{c}_I,$$
$$\mathbf{b}_{II} = -0.025\mathbf{a}_I - 0.510\mathbf{b}_I - 0.859\mathbf{c}_I,$$
$$\mathbf{c}_{II} = 0.998\mathbf{a}_I + 0.033\mathbf{b}_I - 0.048\mathbf{c}_I.$$

For two components, 49.8% and 34.5% of the measured reflections were indexed, respectively, and the reflection overlap was 1.2%.
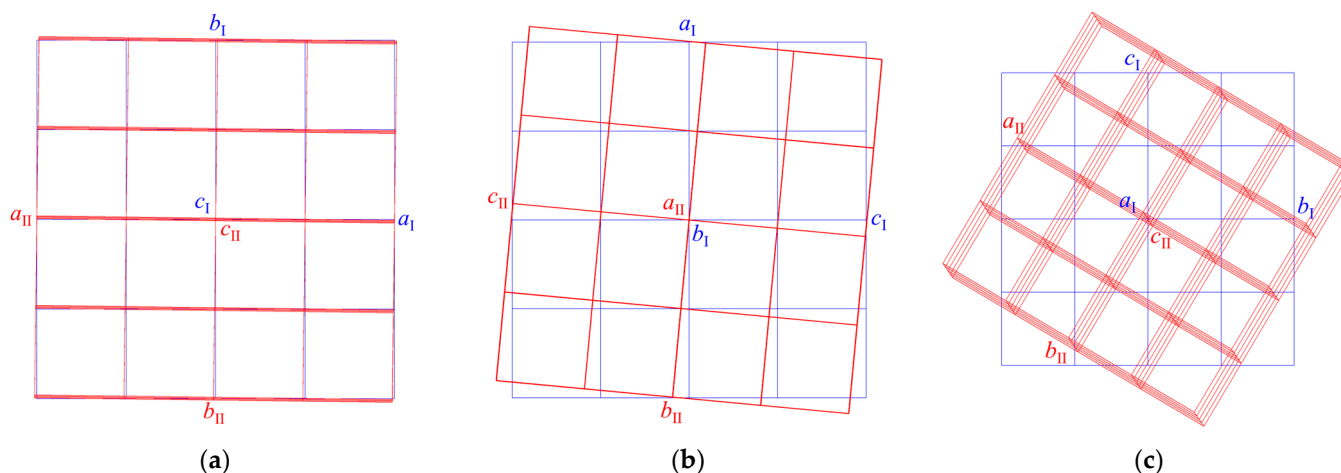

Figure 3. Mutual arrangement of lattices of single-crystal individuals found in the (**a**) first, (**b**) second, and (**c**) third samples.

Reflections from different components were separated into new sets of intensities, and various data reduction options were tested. Complete calculations were carried out for three samples. The best results for the third sample are presented for publication: data reduction was carried out using the reflections from component 1 only and the common scales for two components [25]. All the basic crystallographic calculations (correction for anomalous scattering, averaging of symmetrically equivalent reflections) were performed using the JANA2006 software package (version 20/02/2023) [24]. The atomic structures of the crystals were solved by the charge-flipping method using the Superflip program [26], which is included in the JANA2006 software package. The structural parameters of the

crystals were refined by the full-matrix least squares method. The main crystallographic characteristics and the experimental and structure refinement data are given in Table 1.

Table 1. Experimental details.

Chemical formula	$Na_{0.65}La_{4.35}Mo_3O_{15.81\pm\delta}F_{0.07\pm\varepsilon}$
Crystal system, space group, Z	Cubic, $Pn\bar{3}n$, 4
M	1161.1
T, °C	20
a, Å	11.2366(3)
V, Å^3	1418.75(1)
D, g/cm^3	5.436
Radiation; λ, Å	Mo K_α; 0.71073
μ, mm^{-1}	15.454
Sample size, mm	$0.173 \times 0.11 \times 0.097$
Diffractometer	Xcalibur EosS2
Scan mode	ω
Absorption correction; T_{min}, T_{max}	Gaussian; 0.201, 0.418
θ_{max}, deg	45.23
Ranges of indices h, k, l	$-30 \le h \le 28, -29 \le k \le 30, -27 \le l \le 29$
Numbers of reflections:measured/unique, $R_{int}/I > 3\sigma(I)$	72,997/602, 0.135/465
Refinement method	F-based least squares
Number of parameters	22
$R(|F|)/wR(|F|)$	0.0149/0.0166
S	1.00
$\Delta\rho_{min}/\Delta\rho_{max}$, e Å^{-3}	$-1.00/1.07$

3. Results and Discussion

3.1. Powder X-ray Diffraction and ICP-MS

In accordance with the diffraction pattern of the mixture of the synthesis products (Figure 4), the sample contains two crystalline phases: the desired fluorite-like phase $Na_xLa_{5-x}Mo_3O_{16.5-y}F_y$ as well as the previously studied $Na_5La(MoO_4)_4$ phase [27].
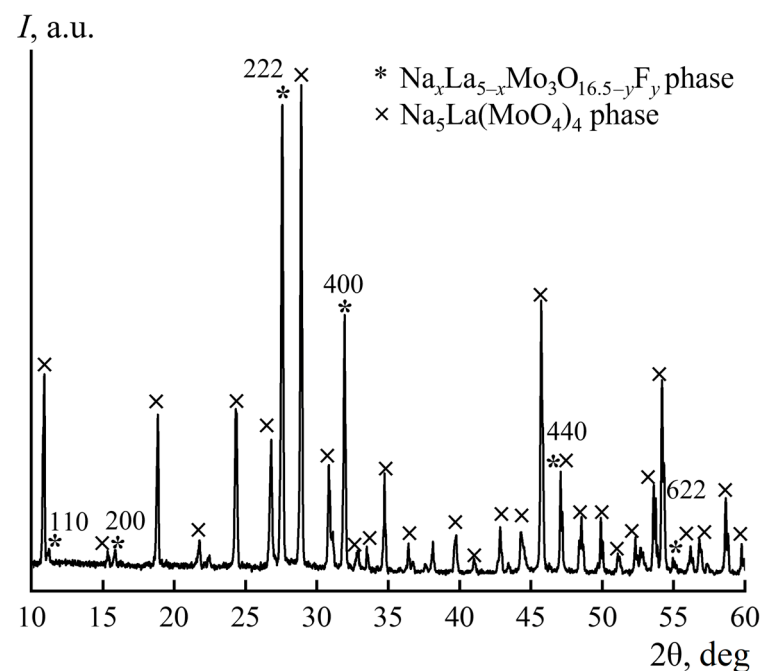

Figure 4. Powder X-ray diffraction pattern of products synthesized in the La_2O_3–MoO_3–NaF system.

Quantitative profile analysis provided the following results. The final total values of the refinement quality parameter and the discrepancy factors for the diffraction profiles were S_p = 2.50, R_p = 14.35%, and R_{pw} = 20.02%. The discrepancy factors were R = 8.02%, R_w = 8.99% for the $Na_xLa_{5-x}Mo_3O_{16.5-y}F_y$ phase and R = 11.91%, R_w = 9.97% for the $Na_5La(MoO_4)_4$ phase. The refined unit cell parameters: a_1 = 11.2344(1) Å, $\alpha_1 = \beta_1 = \gamma_1 = 90°$ for the $Na_xLa_{5-x}Mo_3O_{16.5-y}F_y$ phase and a_2 = 11.5685(1), c_2 = 11.6200(1) Å, $\alpha_2 = \beta_2 = \gamma_2 = 90°$ for the $Na_5La(MoO_4)_4$ phase, which is in good accordance with the experimental data (Table 1) and the literature [27]. The obtained concentrations of the $Na_xLa_{5-x}Mo_3O_{16.5-y}F_y$ and $Na_5La(MoO_4)_4$ phases were 41(2)% and 59(2)%, respectively. It is noteworthy that the sample contained not only the described crystalline phases but also amorphous and poorly crystallized phases, which complicated the interpretation of the results and allowed only qualitative conclusions to be drawn about the yield of the target compounds of the Hubert phases.

To determine the concentration of sodium ions in the $Na_xLa_{5-x}Mo_3O_{16.5-y}F_y$ crystal, three measurements were carried out by the ICP-MS method. The standard deviation did not exceed 5%. The average value was 12,101 µg g^{-1} or 1.21 wt%, which corresponded to a concentration of 1.28 wt% obtained by X-ray diffraction analysis (Table 1).

3.2. Crystal Structure

The unit cell parameters of all three samples obtained in this work correlate with the unit cell parameter of CaF_2 fluorite as $a \approx 2a_f$ (a_f = 5.5 Å). The asymmetric unit of the cell of the cubic modification of the $Na_xLa_{5-x}Mo_3O_{16.5-y}F_y$ crystal contains six atoms. Two La atoms, one Mo atom, and two O atoms occupy the basic crystallographic positions. One O atom is in the interstice. It was localized from the difference Fourier electron density map. This atom is located in a cavity of type II [14] (Wyckoff position 2a in the space group $Pn\bar{3}n$), which is formed by La1 atoms.

After refining the coordinates and the atomic displacement parameters of La1 (12e), La2 (8c), Mo (12d), O1 (16f), and O2 (48i) in the anisotropic approximation and O3 in the isotropic approximation, the difference Fourier maps were calculated near the positions of all the cations. The highest peak (+4.5 e Å^{-3}) and the largest hole (−7.99 e Å^{-3}) of the electron density were observed near the La2 position (Figure 5a). Such a Fourier map shows that the electron density is overestimated in this position and a lighter element can be found in it. Then, the occupancy parameters of the La1, La2, and Mo positions were refined, and a vacancy was found in the position of the La2 atom. After this procedure, the heights of the maximum and minimum of the difference electron density near the La2 position decreased to +3.25 and −3.64 e Å^{-3}, respectively, but the form of the difference Fourier map (Figure 5a) did not change. The sodium atom Na1 was placed in this position. It should be noted that impurity atoms do not enter the crystallographic position of the La1 atom, which agrees with the data obtained for $Ln_5Mo_3O_{16+\delta}$ compounds doped with lead [14], as well as lithium and fluorine [23]. Thus, irrespective of the size of the impurity cation included in the structure of the $Ln_5Mo_3O_{16+\delta}$ compound, it tends to substitute for the rare-earth element only in one of its two positions, $Ln2$. This may be due to the fact that the coordination polyhedron of the La1 atom (four O1 atoms at distances of 2.421(1) Å and four O2 atoms at distances of 2.619(1) Å) is less distorted than the coordination polyhedron of the La2 atom (two O1 atoms at distances of 2.329(1) Å and six O2 atoms at distances of 2.687(1) Å). The occupancy of the La2/Na1 mixed position was refined, assuming that it was 100% occupied. The following values of the site occupancy by lanthanum and sodium atoms in the structure were obtained: 67.4(1)% for La2 and 32.6% for Na1. The difference Fourier map calculated near the mixed La2/Na1 position is shown in Figure 5b.
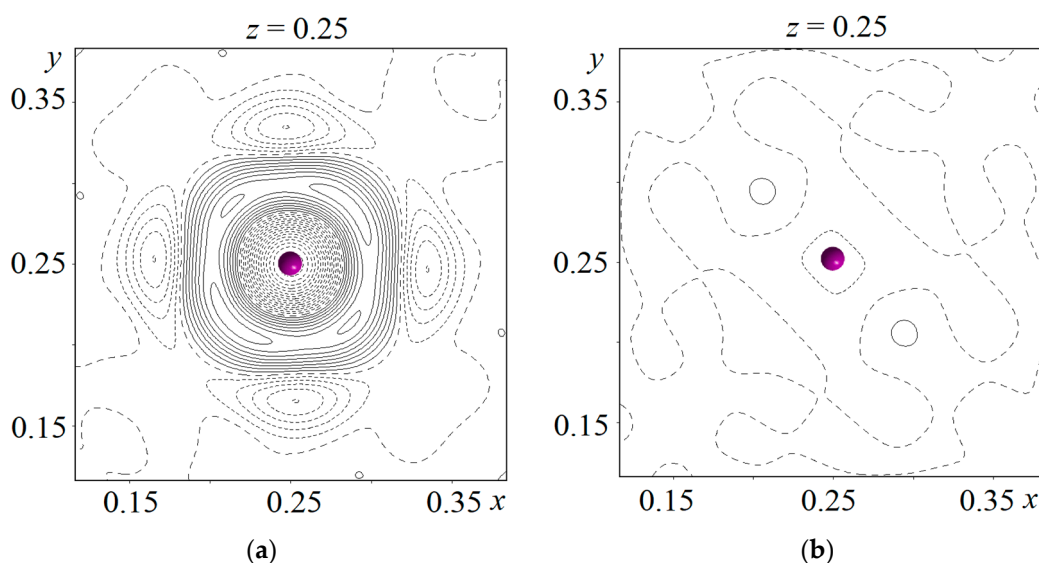
Figure 5. Difference Fourier maps of the electron density near the La2 position: (**a**) Model without sodium atom; (**b**) Model including sodium atom. Isolines are drawn in steps of 0.5 e Å^{-3}. The La2 atom is indicated by a ball.

The total sodium content in the chemical formula was 0.652(2). At this stage of refinement, the chemical formula looked like $Na_{0.652}La_{4.348}Mo_3O_{15.893}$. To fulfill the electrical neutrality condition, some of the oxygen atoms in the sample must be replaced by fluorine atoms in accordance with the chemical formula $Na_xLa_{5-x}Mo_3O_{16.5-y}F_y$. It should be noted that in the structure of all three crystals studied, the special O1 (16*f*) position is occupied with a probability of 100%, while there is a vacancy in the general O2 (48*i*) position. The occupancy of the O3 position (2*a*) is low (~0.15). The fluorine atom was sequentially placed in the O2 and O3 positions. At the final stage of model refinement, the occupancy of the O2 position was 0.984(6) and that of the fluorine atom in the O3 position was 0.14(1). Thus, the chemical formula of the compound can be written as $Na_{0.652(2)}La_{4.348(2)}Mo_3O_{15.811(7)}F_{0.072(7)}$. The sodium impurity concentration in the studied crystals is rather high. This is a consequence of the proximity of the ionic radii of La^{3+} ($R = 1.16$ Å) and Na^+ ($R = 1.18$ Å). In our previous work [23], it was found that a smaller amount of lithium ($R = 0.92$ Å) was included in the molybdate structure ($x = 0.42$), and single crystals were obtained rather than their intergrowths. That is, the formation of such defects is probably caused not only by the growth conditions (the use of ceramic grains as seeds) but also by the concentration of the impurity that replaces the rare-earth element. An analysis of the difference Fourier maps of the electron density calculated at the final stage of refinement of the structural model showed that the highest peaks were located near the positions of the La1, La2, and Mo atoms at distances of ~0.46–0.57 Å.

It is known that in fluorite-like compounds formed in the Ln_2O_3–$Mo(W)O_3$ system, due to high synthesis temperatures, the crystal chemical identity of cations can be leveled, resulting in the "mixing" of Ln and Mo(W) cations over positions [28–30]. The refinement of the structural models of $Nd_5Mo_3O_{16+\delta}$ single crystals [10], and compounds based on them doped with tungsten or lead [12,14], was carried out while taking into account the splitting and partial substitution of molybdenum atoms for neodymium atoms near the Nd position, and also partial substitution of neodymium atoms for molybdenum atoms near the Mo position. Accounting for the mutual substitution of cations led to a decrease in the discrepancy factors and equalization of the peak heights of the residual electron density in all the structures studied. The residual electron density maxima found near oxygen atoms at distances of ~1.5–1.9 Å from the Mo position and ~2.2–2.7 Å from the Nd position indicated a partial displacement of oxygen atoms relative to their main crystallographic positions to ensure the coordination of mutually substituted cations. The low occupancies

of the additional positions of mutually substituted cations result in low occupancies of the positions of the light oxygen atoms coordinating them, complicating their refinement. The presence of high electron density peaks near the La1, La2, and Mo atoms on the final difference Fourier maps of the $Na_xLa_{5-x}Mo_3O_{16.5-y}F_y$ crystal under study suggests that mutual substitutions of cations and additional partially occupied positions of anions are possible in this structure, which, unfortunately, cannot be refined due to the complexity of the structural model. In view of the above, the chemical formula of the studied compound should be written as $Na_{0.65}La_{4.35}Mo_3O_{15.81\pm\delta}F_{0.07\pm\varepsilon}$.

The local change in the atomic configurations found in the structure of oxidized phases of fluorite-like rare-earth molybdates, namely, partial substitution in the cationic sublattice and statistical disordering of all the atoms of the structure, is the basis for the appearance of a continuous network of anion migration paths. The detected interstitial partially occupied positions of the over-stoichiometric anion, which is a free charge carrier, provide the ionic component of the conductivity of the oxidized phases. Thus, the mechanism of ionic conductivity of the oxidized phases of fluorite-like rare-earth molybdates includes the simultaneous participation of both interstitial and lattice oxygen atoms. Undoubtedly, the composition of a crystal affects the partial mutual substitution of cations, the formation of individual complexes, and, as a consequence, its electrical conductivity. In $Nd_5Mo_3O_{16+\delta}$ compounds doped with hexavalent tungsten, the inclusion of interstitial oxygen atoms in the tungsten coordination sphere leads to a decrease in the number of mobile charge carriers, which explains the decrease in conductivity [12]. The heterovalent partial substitution of cations (Nd^{3+} for Pb^{2+}) leads to a decrease in the number of free charge carriers, which results in a decrease in conductivity in compounds doped with lead [14].

The presence of F^- ions in small amounts in the octahedral interstices of the structure under study promotes an increase in oxygen mobility due to additional ionic repulsion between anions of different types. This explains the change in the physical properties of fluorinated molybdates [21,22]. In particular, this makes it possible to understand the reason for the occurrence of a reversible phase transition, which is accompanied by a sharp change in the electrical conductivity and a ferroelectric anomaly in the permittivity in sodium- and fluorine-substituted compounds $NaLn_4Mo_3O_{15}F$ (*Ln* = La, Pr, Nd) [21]. It is interesting to note that a small amount of fluorine in the anionic sublattice affects the transport characteristics of the fluorinated material. For example, it was shown in [18] that for perovskite-related structures doped with fluorine, the mobility of oxygen ions at high fluorine concentrations decreased due to the overlap of the migration paths of diffusion of both anions. Thus, the increase in mobility, rather than the concentration of current carriers, is a decisive factor in improving the conductivity of compounds during their fluorination.

4. Conclusions

Rare-earth molybdates $Na_{0.65}La_{4.35}Mo_3O_{15.81\pm\delta}F_{0.07\pm\varepsilon}$ were obtained for the first time in the single-crystal phase by the flux method. It was found that intergrowths of single-crystal individuals were formed. Such defects may arise due to the growth conditions (two-stage growth using a ceramic grain as a seed) and the concentration of impurity atoms that replace rare-earth atoms. X-ray diffraction analysis of three samples confirmed that the obtained crystals are isostructural to compounds of the $Ln_5Mo_3O_{16+\delta}$ (*Ln* = La–Gd) family of mixed oxygen ion and electronic conductors with a cubic fluorite-like structure. Sodium atoms substitute for lanthanum in one of two positions, centering the more distorted LaO_8 polyhedron. The partial replacement of oxygen atoms by fluorine anions affects the transport characteristics of these compounds by activating oxygen ions due to the effect of additional electrostatic repulsion between anions of different types.

Author Contributions: X-ray diffraction analysis, writing the article, original draft preparation, visualization, translation, data curation, N.E.N.; synthesis of polycrystalline samples, single crystal growth by the flux method, writing the article, original draft preparation, E.I.O.; X-ray diffraction analysis, Rietveld refinement, visualization, A.M.A.; X-ray phase analysis, T.A.S.; ICP-MS analysis, V.B.K.; single crystal growth by the flux method, E.P.K.; X-ray diffraction analysis, writing the article,

original draft preparation, supervision, N.I.S.; writing the article, original draft preparation, as well as reviewing and editing, project administration, O.A.A.; project administration, V.I.V. All authors have read and agreed to the published version of the manuscript.

Data Availability Statement: Cambridge Crystallographic Data Centre. CCDC reference 2278128.

Conflicts of Interest: The authors declare no conflict of interest.

References

1. Hubert, P.H.; Michel, P.; Thozet, A. Structure du molybdate de néodyme $Nd_5Mo_3O_{16}$. *C. R. Hebd. Seances Acad. Sci. Ser. C* **1973**, *276*, 1779–1781.

2. Tsai, M.; Greenblatt, M. Oxide ion conductivity in $Ln_5Mo_3O_{16+x}$ (Ln = La, Pr, Nd, Sm, Gd; x~0.5) with a fluorite-related structure. *Chem. Mater.* **1989**, *1*, 253–259. [CrossRef]

3. Jacas Biendicho, J.; Playford, H.Y.; Rahman, S.M.H.; Norberg, S.T.; Eriksson, S.G.; Hull, S. The fluorite-like phase $Nd_5Mo_3O_{16\pm\delta}$ in the MoO_3–Nd_2O_3 system: Synthesis, crystal structure, and conducting properties. *Inorg. Chem.* **2018**, *57*, 7025–7035. [CrossRef] [PubMed]

4. Istomin, S.Y.; Kotova, A.I.; Lyskov, N.V.; Mazo, G.N.; Antipov, E.V. $Pr_5Mo_3O_{16+\delta}$: A new anode material for solid oxide fuel cells. *Russ. J. Inorg. Chem.* **2018**, *63*, 1291–1296. [CrossRef]

5. Lyskov, N.V.; Kotova, A.I.; Istomin, S.Y.; Mazo, G.N.; Antipov, E.V. Electrochemical properties of electrode materials based on $Pr_5Mo_3O_{16+\delta}$. *Russ. J. Electrochem.* **2020**, *56*, 93–99. [CrossRef]

6. Lyskov, N.V.; Kotova, A.I.; Petukhov, D.I.; Istomin, S.Y.; Mazo, G.N. A new electroactive and stable electrode based on praseodymium molybdate for symmetrical SOFCs. *Russ. J. Electrochem.* **2022**, *58*, 989–997. [CrossRef]

7. Fournier, J.P.; Kohlmuller, R. Étude des phases $MLn_4Mo_3O_{16}$ et $M'Ln_6Mo_4O_{22}$ (M = Cd; M' = Ca, Sr) de structure dérivée de la fluorine par magnétochemie, luminescence cristalline, spectroscopie infrarouge, et radiocristallographie. Hypothèse structurale pour la phase $CdTm_4Mo_3O_{16}$. *Rev. Chim. Miner.* **1971**, *8*, 241–276.

8. Bourdet, J.-B.; Chevalier, R.; Fournier, J.P.; Kohlmuller, R.; Omaly, J. A structural study of cadmium yttrium molybdate $CdY_4Mo_3O_{16}$. *Acta Crystallogr. B* **1982**, *38*, 2371–2374. [CrossRef]

9. Martinez-Lope, M.J.; Alonso, J.A.; Sheptyakov, D.; Pomyakushin, V. Preparation and structural study from neutron diffraction data of $Pr_5Mo_3O_{16}$. *J. Solid State Chem.* **2010**, *183*, 2974–2978. [CrossRef]

10. Alekseeva, O.A.; Gagor, A.B.; Pietraszko, A.P.; Sorokina, N.I.; Bolotina, N.B.; Artemov, V.V.; Kharitonova, E.P.; Voronkova, V.I. Crystal structure of the oxygen conducting compound $Nd_5Mo_3O_{16}$. *Z. Kristallogr.* **2012**, *227*, 869–875. [CrossRef]

11. Vu, T.D.; Krichen, F.; Barre, M.; Busselez, R.; Adil, K.; Jouanneaux, A.; Suard, E.; Goutenoire, F. Crystal structure and ion conducting properties of $La_5NbMo_2O_{16}$. *J. Solid State Chem.* **2016**, *237*, 411–416. [CrossRef]

12. Antipin, A.M.; Sorokina, N.I.; Alekseeva, O.A.; Zubavichus, Y.V.; Artemov, V.V.; Kharitonova, E.P.; Orlova, E.I.; Voronkova, V.I. Structure of $Nd_5Mo_3O_{16+\delta}$ single crystals doped with tungsten. *Crystallogr. Rep.* **2018**, *63*, 339–343. [CrossRef]

13. Faurie, J.-P. Préparation de nouvelles phases $MLn_4Mo_3O_{16}$, $MLn_6Mo_4O_{22}$ de structure dérivée du type fluorine. *Bull. Soc. Chim. Fr.* **1971**, *11*, 3865–3868.

14. Antipin, A.M.; Sorokina, N.I.; Alekseeva, O.A.; Kharitonova, E.P.; Orlova, E.I.; Voronkova, V.I. Crystal structure of fluorite-like compound based on $Nd_5Mo_3O_{16}$ with lead partly substituting for neodymium. *Acta Crystallogr. B* **2015**, *71*, 186–193. [CrossRef]

15. Tarasova, N.A.; Filinkova, Y.V.; Animitsa, I.E. Electric properties of oxyfluorides $Ba_2In_2O_{5-0.5x}F_x$ with brownmillerite structure. *Russ. J. Electrochem.* **2013**, *49*, 45–51. [CrossRef]

16. Tarasova, N.A.; Animitsa, I.E. Effect of anion doping on mobility of ionic charge carriers in solid solutions based on $Ba_2In_2O_5$. *Russ. J. Electrochem.* **2013**, *49*, 698–703. [CrossRef]

17. Tarasova, N.; Animitsa, I. Novel proton-conducting oxyfluorides $Ba_{4-0.5x}In_2Zr_2O_{11-x}F_x$ with perovskite structure. *Solid State Ionics* **2014**, *264*, 69–76. [CrossRef]

18. Tarasova, N.; Animitsa, I. The influence of fluorine doping on transport properties in the novel proton conductors $Ba_4In_2Zr_2O_{11-0.5x}F_x$ with perovskite structure. *Solid State Sci.* **2019**, *87*, 87–92. [CrossRef]

19. Glumov, O.V.; Bodhar, V.A.; Mel'nikova, N.A.; Yakobson, V.E.; Murin, I.V. Electrical conductivity of potassium titanyl phosphate $KTiOPO_4$ pure crystals and those doped with Na^+, Rb^+, and F^- ions. *Russ. J. Electrochem.* **2017**, *53*, 846–851. [CrossRef]

20. Ushakov, A.E.; Merkulov, O.V.; Markov, A.A.; Patrakeev, M.V.; Leonidov, I.A. Ceramic and transport properties of halogen-substituted strontium ferrite. *Ceram. Int.* **2018**, *44*, 11301–11306. [CrossRef]

21. Voronkova, V.; Kharitonova, E.; Orlova, E.; Kezionis, A.; Petrulionis, D. Effect of sodium and fluorine co-doping on the properties of fluorite-like rare-earth molybdates of $Nd_5Mo_3O_{16}$ type. *Eur. J. Inorg. Chem.* **2019**, *2019*, 1250–1256. [CrossRef]

22. Orlova, E.I.; Sorokin, T.A.; Baldin, E.D.; Zakharova, E.Y.; Kharitonova, E.P.; Lyskov, N.V.; Yapaskurt, V.O.; Voronkova, V.I. The fluorite-like $LiSm_4Mo_3O_{15}F$ ceramics: Synthesis and conductivity. *J. Solid State Chem.* **2023**, *324*, 124078. [CrossRef]

23. Orlova, E.I.; Sorokin, T.A.; Kvartalov, V.B.; Antipin, A.M.; Novikova, N.E.; Kharitonova, E.P.; Sorokina, N.I.; Alekseeva, O.A.; Voronkova, V.I. Rare-earth fluorite-like $Li_{0.42}La_{4.58}Mo_3O_{15.76\pm\delta}F_{0.42\pm\varepsilon}$ molybdates: Crystal growth and atomic structure. *Crystals* **2023**, *13*, 1009. [CrossRef]

24. Petříček, V.; Dušek, M.; Palatinus, L. Crystallographic computing system JANA2006: General features. *Z. Kristallogr.* **2014**, *229*, 345–352. [CrossRef]

25. Rigaku Oxford Diffraction. *CrysAlisPro Software System, Version 42.74a*; Rigaku Corporation: Oxford, UK, 2018.

26. Palatinus, L. The Charge-flipping algorithm in crystallography. *Acta Crystallogr. B* **2013**, *69*, 1–16. [CrossRef] [PubMed]

27. Efremov, V.A.; Trunov, V.K.; Berezina, T.A. On fine changes in the structure of scheelite-like $Na_5La(MoO_4)_4$ upon variation of their elemental composition. *Kristallografiya* **1982**, *27*, 134–139. (In Russian)

28. Klevtsov, P.V.; Kharchenko, L.Y.; Klevtsova, R.F. On crystallization and polymorphism of Ln_2MoO_6 type rare-earth oxymolybdates. *Kristallografiya* **1975**, *20*, 571–578. (In Russian)

29. Magraso, A.; Hervoches, C.H.; Ahmed, I.; Hull, S.; Nordström, J.; Skilbred, A.W.B.; Haugsrud, R. In situ high temperature powder neutron diffraction study of undoped and Ca-doped $La_{28-x}W_{4+x}O_{54+3x/2}$ ($x = 0.85$). *J. Mater. Chem. A* **2013**, *1*, 3774–3782. [CrossRef]

30. Evdokimov, A.A.; Efremov, V.A.; Trunov, V.K.; Kleinman, I.A.; Dzhurinsky, B.F. *Compounds of Rare Earth Elements. Molybdates, Tungstates*; Nauka: Moscow, Russia, 1991; 267p. (In Russian)